Correlated excitations and Raman scattering in glasses

Richard M. Martin and Frank L. Galeener
Xerox Palo Alto Research Centers, 3333 Coyote Hill Road, Palo Alto, California 94304
(Received 21 March 1980)

The dominant Raman line in AX_2 tetrahedral glasses is demonstrated to be caused by correlated symmetric stretch motions of the bridging X atoms. Using a bond-polarizability model and the central-force model of Sen and Thorpe, we derive simple analytic forms for Raman spectra. We show that correlations may cause qualitative changes in the *polarized* spectrum leading to a peak at the *edge* of a band of vibrational states, whereas the depolarized spectrum is less affected and mimics the density of states. Both features are clearly observed in GeO_2 and explain features in many other glasses. The same reasoning leads to a prediction of unusual spectral features in electronic spectra of disordered solids which may be observable in angular-dependent photoemission.

I. INTRODUCTION

Vibrational properties of glasses have been studied extensively by Raman and infrared spectroscopy. A survey of the data for a large number of covalent network glasses,[1-10] such as SiO_2,[1,2] GeO_2,[2,3] and P_2O_5,[8] reveals several ubiquitous features. One is that the Raman spectra of each glass are dominated by a single peak which is highly polarized, i.e., it is strong when the incident- and scattered-light polarization vectors are parallel (HH) but weak when they are perpendicular (HV). This peak is usually an order of magnitude more intense than any other and comprises more than 50% of the HH spectrum. The depolarized HV spectrum has very different structure with several peaks having a close correspondence[2] to the TO and LO modes determined from infrared spectroscopy. Striking sharp features also appear in the HH Raman spectra of other disordered materials such as amorphous As,[11,12] and P.[13] These "selection rules," which cause different vibrational modes to be weighted very differently in the various experimental probes, are the subject of the present work.

In this paper we analyze the nature of Raman scattering in network glasses. Our primary result is that polarized HH spectra are greatly affected by correlations in the motion of nearby atoms. It follows that analysis of the Raman peaks is meaningful only if the correlations in the extended network are taken into account and, conversely, the polarized spectra provide information on the correlations. On the other hand, the depolarized HV spectra are shown to resemble the density of states weighted by smoothly varying factors, as has been observed experimentally.[1-11,14] We give explicit calculations and comparison with experiment for vitreous GeO_2, for which there is an unambiguous indentification of the salient features of the Raman spectra[1] and density of states as measured by neutron scattering.[14] Finally we show that the ideas can be applied to other network glasses and to other properties of amorphous systems and we make a prediction of unusual structure in angular-dependent photoemission in amorphous tetrahedral semiconductors such as a-Si.

The primitive state of the current understanding of the vibrational and electronic properties of glasses compared to that for crystals can be attributed to the difficulty of deriving unique theoretical predictions for excitations in disordered systems.[15,16] In network glasses the situation is particularly complex because there is much evidence[17] that local structural order is preserved, nevertheless, the local units are strongly coupled into a topologically disordered network. Theoretical approaches toward this problem have divided into various categories. (i) The simplest is the molecular approximation[18,19] in which the coupling between the local units is ignored. This may be adequate in special cases where the coupling is small, but here we are interested in the cases where coupling in the network is nontrivial and cannot be ignored. (ii) Coupling can be accounted for in quasicrystalline calculations,[19] but there the disorder is included in an unsatisfactory heuristic manner. (iii) The states of a disordered network may be addressed directly by numerical calculations on large clusters.[16,20-22] Such methods are very powerful, but they involve large computations and are sensitive to the assumptions concerning the structure and the boundary conditions. (iv) Numerical calculations[23,24] on small clusters with self-consistent Bethe lattice-boundary conditions reduce the computational problems but have the same difficulty as the larger cluster calculations so that the form of the solution is not transparent. (v) Finally, the study of approximate Hamiltonians in topologically disordered systems[25-27] has provided simple analytic results for bounds on the excitation bands and the nature of the eigenstates. This method takes into account both local order and

strong coupling through the disordered network, which are the two essential ingredients to understanding the Raman spectra.

Galeener[10] has shown that the central force Bethe-lattice calculations of Sen and Thorpe[27] (ST) are in quantitative agreement with large cluster calculations for 4-2 connected AX_2 glasses, and has used the results to provide a new interpretation of the frequency and atomic motions of the dominant Raman line in SiO_2, GeO_2, and BeF_2. We shall utilize these methods and results here, and will extend the treatment of Raman scattering to include broadening due to quantitative disorder and the inclusion of noncentral bond-bending forces.

In Sec. II we briefly describe the structure and vibrational spectra of network glasses with emphasis upon GeO_2. In Sec. III we analyze the Raman process and give expressions for the correlation functions required in polarized and depolarized Raman spectra. Application of the central force model to AX_2 glasses is discussed and extended in Sec. IV, with a specific treatment of GeO_2. Comments on application to other systems and excitations and conclusions are given in Sec. V.

II. STRUCTURE AND VIBRATIONAL MODES OF GLASSES: GeO_2

Experimental studies[17,28] have shown that glasses such as SiO_2, GeO_2, etc., are formed with strong covalent bonds which preserve the local coordination and bond angles in a topologically disordered network. The network is continuous and extended so that there are no isolated molecular units. A widely accepted model for such a structure is the continuous random network (CRN).[17,29] CRN models have been constructed for many systems satisfying the above conditions. The uncertainty in these models is the degree to which there is medium-range order, such as angular correlations manifested in preferred dihedral angles—an aspect which has not been successfully determined experimentally.[28] We will proceed with the CRN model for a glass, bearing in mind the uncertainties in the medium-range order.

The structure of an AX_2 4-2 coordinated glass is illustrated in Fig. 1. There is shown a part of an extended network in which every atom of a given type has similar coordination. An example is GeO_2, for which x-ray studies[28] indicate that every Ge is surrounded by four O atoms at the corners of a nearly regular tetrahedron, and every O atom bridges between two Ge atoms. There is only a small spread in the Ge—O distance $d \sim 1.74$ Å and in the Ge-O-Ge angle θ whose mean value is $\sim 133°$. From the radial densities given in Ref. 28, we estimate the angular spread to be $133° \pm 3°$, but this is very uncertain as pointed out by the authors of Ref. 28. The

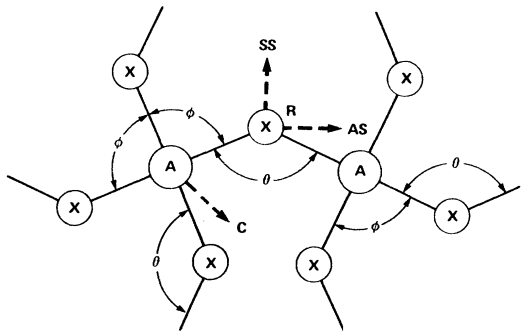

FIG. 1. Schematic illustration of the AX_2 local atomic order, for example SiO_2 or GeO_2. This is the building block from which either a crystal or a random-network glass is constructed. The symmetric stretch (SS) and asymmetric stretch (AS) X motions are shown, as well as a general cation (C) motion.

"ring statistics" of this continuous random network are not known but may be similar to those of SiO_2.[30]

The reduced HH and HV Raman spectra[2,10] of v-GeO_2 are shown in Fig. 2(a). It can be seen that the dominant line in the HH spectrum is highly polarized, exhibiting little strength in the HV spectrum, while the HV spectral features are nearly unpolarized, appearing with about the same strength in both spectra. Galeener and Lucovsky[2] compared the Raman and infrared (ir) spectra and concluded that the features marked TO-LO are to be interpreted as transverse optical-longitudinal optical pairs. Each TO-LO pair is viewed as arising from a single "bare" mode, calculated using a theory that does not include the long-range dipolar forces which lead to TO-LO splitting.

The frequencies of the observed Raman and ir peaks were analyzed by Galeener[10] in terms of the idealized central force model of Sen and Thorpe.[27] The density of bare-mode vibrational states which was deduced from that model is shown schematically in Fig. 2(b). There are two bands of vibrational states, bounded by the frequencies ω_1, ω_2, ω_3, and ω_4 for which simple formulas are available.[10,27] There is a δ function at the upper frequency edge of each of these bands, and each δ function was assumed to correspond to a TO-LO pair. On this assumption it was found that the computed position of the lowest band edge (ω_1) corresponded rather well with the observed position of the dominant Raman line in several tetrahedral glasses. This correspondence is illustrated for v-GeO_2 by the dashed vertical line drawn downward from the dominant Raman peak in Fig. 2. The single state at the band edge ω_1 in the ST theory corresponds to the symmetric stretch (SS in Fig. 1) motion of all X atoms precisely along the bisector of the bridging angle θ, the A atoms remaining at rest. Thus Galeener[10] argued

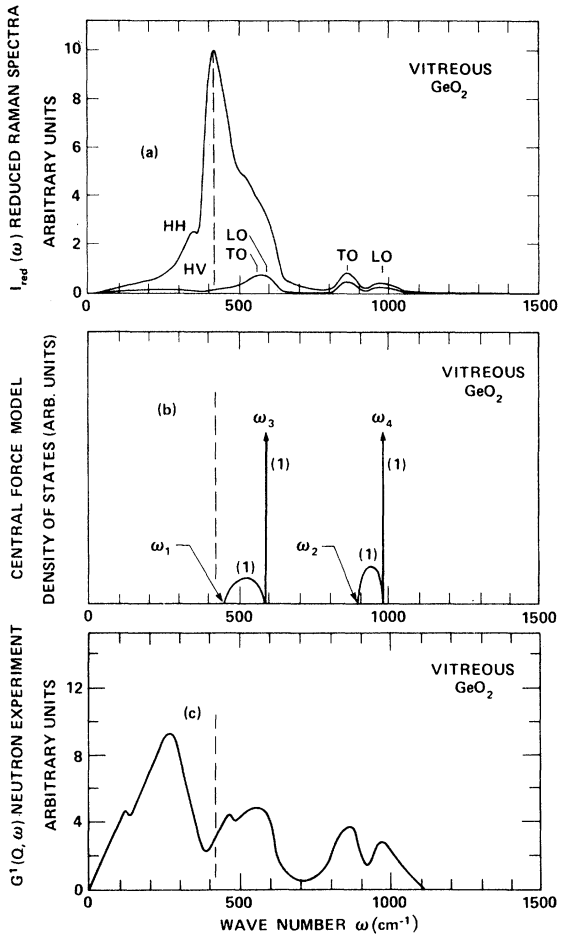

FIG. 2. Spectra of vitreous GeO_2. (a) Reduced Raman spectra from Ref. 2. (b) Schematic density of states from the Sen-Thorpe central-force model as applied in Ref. 10. (c) Neutron measurements of the vibrational density of states from Ref. 14. The dotted line shows the relation of the dominant Raman peak to the band edge in (b) and the minimum in the experimental density of states (c).

that the SS motion at the band edge accounts for the dominant Raman line. In Secs. III and IV we shall give a detailed analysis of a glass with topological and quantitative disorder and we shall *derive* this assignment of the Raman scattering to the SS mode at the band edge.

The inference that the dominant Raman line in v-GeO_2 lies near a band edge is corroborated by new experimental results[14] shown in Fig. 2(c). Here, we present the results of inelastic neutron scattering studies of v-GeO_2, where $G^1(Q,\omega)$ is the first-order single-phonon contribution to the reduced neutron scattering spectrum and can be shown to be a good measure of the total vibrational density of states (VDOS). The small peaks at ~ 115 and ~ 460 cm^{-1} should be ignored in the present discussion; they may arise from experimental noise (not shown).[14] The position of the dashed line in Fig. 2(c) shows clearly that the dominant Raman line does not occur at a peak in the density of states. The Raman line at 420 cm^{-1} is very near a minimum in the VDOS, and in view of the central force analysis it is reasonable to associate the Raman line with the low-frequency edge of the band of states which peaks at $\simeq 560$ cm^{-1}.

An additional observation comes from comparison of Figs. 2(a) and 2(c). There are four maxima in the HV Raman spectra, at approximately 260, 570, 860, and 970 cm^{-1}. These peaks correspond quite closely to the four major peaks in the neutron-determined VDOS in Fig. 2(c). The HV Raman peaks appear to be somewhat narrower than the corresponding ones in the VDOS, and their relative strengths are different than in the VDOS. Nevertheless one can see that a linear combination of four subbands taken from the VDOS can be made to provide a convincing representation of the HV Raman spectrum. With this meaning, we say that the HV Raman spectrum "mimics" the density of states, while the dominant part of the HH spectrum is qualitatively different from the density of states.

Vibrational modes of corresponding crystals may be used to test the above interpretations. The displacement patterns for α- and β-quartz crystals have been derived by Bates.[31] In β quartz there is only one A mode and an analysis of Bates's results shows that this mode consists precisely of SS oxygen motion, as defined in Fig. 1. Experimentally this mode gives strong polarized Raman scatttering at 462 cm^{-1} in β quartz,[32] which lends strong support to our contention that essentially the same modes are responsible for the strong polarized Raman feature in vitreous SiO_2 (Refs. 1 and 2) which peaks at ~ 430 cm^{-1}. In α quartz the symmetry is lower so that there are other A modes but the one which is strongest in the Raman spectrum[33] is present at almost exactly the same frequency (464 cm^{-1}) as the A mode in the β form. In GeO_2 there are available[34] Raman spectra of crystals with the α-quartz structure which show that there is one strong Raman mode at 440 cm^{-1} very near the position of the single strong polarized Raman mode found at ~ 420 cm^{-1} in the glass. In addition, the Raman data of Ref. 34 show that the bond-bending modes in GeO_2 shift to lower energies relative to SiO_2, as expected from the heavier Ge mass, so that all except the very highest frequency LO bond-bending modes are lower in frequency than the strong A_1 SS Raman mode. This fortunate occurrence gives rise to a separation of bond-bending and SS modes in GeO_2. This is the origin of the pronounced dip in the density of states observed by neutron scattering on polycrystalline α-GeO_2 (the polycrystalline data[14] are very similar to the glass data[14] shown in Fig. 2). It is this feature that allows the atomic motions corresponding to the A_1 mode in the

crystal to persist in vitreous GeO_2 with less broadening than in vitreous SiO_2.

The Raman spectra of other glasses show very similar features. These include the tetrahedral AX_2 glasses SiO_2,[1,2] BeF_2,[4] GeS_2,[5] and $ZnCl_2$.[6] The spectra of SiO_2 appear to resemble GeO_2 in every way except that the low-frequency bond-bending modes are more mixed with the SS modes so that the features are not as cleanly separated as in GeO_2. Pyramidal glasses such as As_2O_3,[7] As_2Se_3,[7] and P_2O_5,[8] and B_2O_3 (Ref. 9) also have a strong polarized feature with similar characteristics. A recent work by Thorpe and Galeener[35] extends the central force model to pyramidal glasses, and it can be shown that a correlated SS motion is found at a lower band edge, just as in the tetrahedral glasses. Therefore all our conclusions can be carried over immediately to these glasses as well.

III. POLARIZATION SELECTION RULES AND CORRELATIONS IN GLASSES

In this section we consider Raman scattering from the vibrational excitations of a network glass. The crux of the problem is taking into account correlations among different atoms in the disordered network. We show that the correlations dramatically affect polarized Raman scattering, giving structure in the spectrum very different from that in the density of states. The depolarized Raman spectrum is much less affected and in general closely resembles the density of states. Our mathematical analysis uses the tools developed for disordered crystals[15] but with rather different physical results. The importance of correlations for Raman scattering has been recognized by many workers,[19–27] but to our knowledge has been explored only by numerical simulations for specific model clusters.[21,22,24]

Raman scattering is a long-wavelength experimental probe which measures the fluctuations in the dielectric function. The spectral intensity is given by the imaginary part of the dynamic correlation function[36,37]

$$S_{ij}(q,\omega) = -\,\mathrm{Im}\int dr\,dr' e^{iq(r-r')} \times \int dt\, e^{i\omega t}\langle \delta\epsilon_{ij}(r,t)\delta\epsilon_{ij}(r',0)\rangle \ , \quad (1)$$

where i and j are the incident and scattered light polarization directions. The actual Raman intensities are proportional to the S_{ij} and in an isotropic system the two independent spectra are often denoted $I_{HH}(\omega) \propto S_{ii}(\omega)$ and $I_{HV}(\omega) \propto S_{ij}(\omega)$, $i \neq j$. We will ignore the wave vector of light so that $q \approx 0$ in which case the dependence of $\delta\epsilon_{ij}$ on r may be suppressed. To linear order the dielectric fluctuations are proportional to the atomic displacements u_k^l, where l denotes the atom and k the vector direction

$$\delta\epsilon_{ij}(t) = \frac{\partial\epsilon_{ij}}{\partial u_k^l} u_k^l(t) \equiv \epsilon_{ij,lk} u_k^l(t) \ . \quad (2)$$

Then S is given by

$$S_{ij}(\omega) = -\sum_{\substack{ll'\\kk'}} \epsilon_{ij,lk}\epsilon_{ij,l'k'}\,\mathrm{Im}\int dt\, e^{i\omega t}\langle u_k^l(t)u_{k'}^{l'}(0)\rangle \ , \quad (3)$$

which involves the thermal average correlation function for displacements of atoms at sites l and l' which may in principle be any sites in the extended network.

It will be convenient to use the relation of the correlation function to the causal Green's function to cast the scattering spectrum in the form[36,38–40]

$$S_{ij}(\omega) = -\frac{2\omega}{1-e^{\beta\omega}} \sum_{\substack{ll'\\kk'}} \epsilon_{ij,lk}\epsilon_{ij,l'k'}\,\mathrm{Im}G_{kk'}(l,l',\omega+i0^+) \ . \quad (4)$$

Here the first factor contains the thermal Bose factors, the Green's function contains all information on correlations, and 0^+ denotes a positive infinitesimal which defines the position of poles in the complex plane. The reduced Raman spectrum[40,41] is defined by dividing out the Bose factors so that it involves only the polarizability derivatives and Green's function in Eq. (4). The vibrational density of states is given by[15,38,39]

$$\rho(\omega) = -\frac{\omega}{\pi}\,\mathrm{Im}\sum_{lk} G_{kk}(l,l,\omega+i0^+) \ . \quad (5)$$

Comparison of Eqs. (4) and (5) shows that the reduced Raman spectrum differs from the density of states for two reasons: (i) the derivatives of the dielectric function weight differently the various types of atomic motions. This factor alone gives a weighted density of states, i.e., a smoothly[40,41] varying function multiplying $\rho(\omega)$ in the spectral intensity, discussed extensively in the literature. (ii) The Raman spectrum involves a sum over all pairs of atoms and is modified by correlations in displacements of different atoms.

It is useful to divide the fluctuations in the dielectric function into isotropic and anisotropic parts[37,42] $\delta\epsilon_{ij} = \delta\epsilon^0 + \delta\epsilon_{ij}$ where $\delta\epsilon^0$ is a scalar and is one-third the trace of the fluctuation in the dielectric tensor and $\delta\epsilon_{ij}$ is traceless. In molecular systems these two parts give, respectively, polarized and depolarized Raman scattering.[37,42] We shall see that in a network glass the same polarization rules hold and that the effect of correlations is very different in polarized versus depolarized scattering.

In order to derive explicit results we use a bond polarizability model as has been defined by Bell and Hibbins-Butler[21] for the AX_2 glasses. This model has been used in cluster calculations[21,24] of Raman cross sections so that our results can be compared. The dielectric function is given by

$$\epsilon_{ij} = 1 + \frac{1}{\Omega}\sum_m [\alpha^m\delta_{ij} + \beta^m(n_i^m n_j^m - \tfrac{1}{3}\delta_{ij})] \ . \quad (6)$$

Here n^m is a unit vector along bond m, α^m is the isotropic polarizability, and β^m the magnitude of the anisotropic part. This form has also been used to analyze Raman spectra of α quartz.[43] If we assume α^m and β^m depend only upon the length r^m of bond m, then the derivatives may be written

$$\frac{\partial \epsilon_{ij}}{\partial u_k^l} = \frac{1}{\Omega} \sum_m{}' [\alpha'^m n_k^m \delta_{ij} + \beta'^m n_k^m (n_i^m n_j^m - \tfrac{1}{3}\delta_{ij}) + \frac{\beta^m}{r^m}(n_i^m \delta_{jk} + n_j^m \delta_{ik} - 2 n_i^m n_j^m n_k^m)] \ , \tag{7}$$

where the sum is restricted to the bonds m attached to atom 1, $\alpha'^m = \partial\alpha^m/\partial r^m$, $\beta'^m = \partial\beta^m/\partial r^m$, and $\vec{n}^m$ is defined as the bond vector directed toward atom l.

We first discuss the polarized scattering which results from the isotropic δ_{ij} first term in Eq. (7). The polarized spectrum given by Eqs. (3) and (7) is

$$S^p(\omega) = -\sum_{ll'} \sum_{mm'} \alpha'^m \alpha'^{m'} \mathrm{Im} \int dt\, e^{i\omega t} \langle \vec{n}^m \cdot \vec{u}^l(t) \times \vec{n}^{m'} \cdot \vec{u}^{l'}(0) \rangle \ , \tag{8}$$

where m denotes all bonds attached to atom l, etc. The scalar dot product in Eq. (8) projects out the bond-stretching components of the displacements and the polarized scattering is a sum over all correlated bond-stretching motions weighted by the scalar polarizability derivatives α'^m. The important point is that α'^m has a nonzero mean value for each type of bond in the system. Let us specialize with one type of bond and write

$$\alpha'^m = \alpha' + \delta\alpha'^m \ , \tag{9}$$

where α' is the mean derivative and $\delta\alpha'^m$ is the fluctuating part. Then the expression for polarized scattering becomes

$$S^p(\omega) = -(\alpha')^2 \mathrm{Im} \int dt\, e^{i\omega t} \sum_{ll'} \sum_{mm'} \langle n^m \cdot u^l(t) \times n^{m'} \cdot u^{l'}(0) \rangle + \cdots \ , \tag{10}$$

where the ellipsis represents terms involving $\delta\alpha'^m$.

The portion of the scattering given in Eq. (10) is simply a sum over all correlated bond-stretching displacements. Sen and Thorpe[27] (ST) have shown that these displacements may be highly correlated on different sites, in which case Eq. (10) is qualitatively different from the density of states. On the other hand, the fluctuations $\delta\alpha'^m$ are not expected to be correlated on different bonds; therefore, the remaining polarized scattering involving the $\delta\alpha'^m$ is expected to closely resemble the weighted bond-stretching density of states. We will give explicit results for a 4-2 coordinated AX_2 network glass in the next section using an extension of the ST model.

Depolarized scattering gives qualitatively different results. To see the overall effects, consider a typical term

$$S_{ij}^{dp}(\omega) = -\sum_{ll',mm'} \beta'^m \beta'^m (n_i^m n_j^m - \tfrac{1}{3}\delta_{ij}) \times (n_i^{m'} n_j^{m'} - \tfrac{1}{3}\delta_{ij}) \times \mathrm{Im} \int dt\, e^{i\omega t} \langle \vec{n}^m \cdot \vec{u}^l(t) \times \vec{n}^{m'} \cdot \vec{u}^{l'}(0) \rangle \ . \tag{11}$$

The important aspect of Eq. (11) is that it involves the correlation of displacements with the static bond directions n^m and $n^{m'}$. The expectation values in Eq. (11) depend only upon the relative orientations of the bond and displacement vectors whereas the first terms in brackets depend upon the orientation of the vectors n^m and $n^{m'}$ relative to the laboratory Cartesian coordinate system. In an extended isotropic network the sums over all bonds in Eq. (11) will average over all possible orientations, in particular, we may say that vector n^m may adopt any orientation with equal probability and the plane defined by the two vectors n^m and $n^{m'}$ may have any orientation. However, if there is angular correlation in the glass there may be a preferred distribution of angles $\phi_{mm'}$ between the two vectors. For example, it is generally found that angles between neighboring bonds have only a small distribution around some energetically favored bond angle.

The average over all orientations for the bracketed terms in Eq. (11) for a fixed $\phi_{mm'}$ can be shown to obey the simple relation

$$\langle (n_i^m n_j^m - \tfrac{1}{3}\delta_j)(n_i^{m'} n_j^{m'} - \tfrac{1}{3}\delta_{ij}) \rangle = \tfrac{2}{3}(\cos^2\phi_{mm'} - \tfrac{1}{3}) \langle (n_i^m n_j^m - \tfrac{1}{3}\delta_{ij})^2 \rangle \ . \tag{12}$$

That is, all averages over different bonds in Eq. (11) can be related by the proportionality factor on the right-hand side of Eq. (12) to a self-correlation function which is well known.[42] The same can be shown straightforwardly to hold for all depolarized terms arising from the bond polarizability equations (7).

One important result of our derivation is that the two independent depolarized spectra are always related by $S_{ii}^{dp}(\omega) = (\frac{4}{3}) S_{ij}^{dp}(\omega)$ for $i \neq j$. This follows

from the well-known result for a single bond[42] and the fact that angular averages for every term in the expression for depolarized scattering can be related to the single-bond averages via Eq. (12). The actual Raman intensities I_{HH} and I_{HV} can therefore be combined to define an isotropic scalar scattering

$$I_p(\omega) \equiv I_{HH}(\omega) - \tfrac{4}{3} I_{HV}(\omega) \propto S^p(\omega) \ , \qquad (13)$$

which involves only the isotropic components of the local bond polarizabilities. The depolarized part $I_{HV}(\omega) \propto S_{ij}^{dp}(\omega)$, $i \neq j$, is the anisotropic counterpart involving only the anisotropic components of the bond polarizabilities.

The second important result is the very different effect of correlations upon the polarized and depolarized spectra. The polarized spectra may be greatly modified by correlations because of the sum in Eq. (10), which runs over all pairs of atoms in the network. Any correlations of stretching motions of nearby atoms will affect the spectrum increasing the scattering strength of modes with in-phase motion at similar sites. On the other hand, the correlation functions for depolarized scattering involve the factor $(\cos^2\phi_{mm'} - \frac{1}{3})$ in Eq. (12). This factor is always less than $\frac{2}{3}$, can have either sign, and averages to zero for uncorrelated distribution of all possible values of $\phi_{mm'}$. In a glass one expects, at most, short-range correlations in the angles. Then the weighting factor in Eq. (11) is nonzero only for near neighbors and is in general considerably reduced from unity. In the absence of more detailed information, the most reasonable starting point is to assume no correlations whatsoever. Then the depolarized spectrum of Eq. (11) involves only self-correlations and is proportional to the density of states multiplied by smoothly varying functions which account for the change in the various types of atomic displacements with frequency. In this sense we expect depolarized scattering to "mimic" the density of states.[40]

A corrollary of this section is that short- and medium-range angular correlations, such as preferred dihedral angles, can lead to pronounced differences in the depolarized spectrum from the density of states. (Indeed, a crystal has long-range order in the angular orientations so that depolarized scattering involves long-range correlations to the same degree as does the polarized scattering.) Therefore one should look for anomalies in the depolarized scattering to find evidence for medium-range order in a glass. This area needs further experimental and theoretical study.

IV. RAMAN SCATTERING IN AX_2 GLASSES

In this section we consider in detail the correlation functions needed to evaluate the expression for Raman cross section derived in the previous section in the special case of the 4-2 coordinated AX_2 glasses. The starting point for our analytical approach is the characterization of systems having "topological disorder" by Weaire and Thorpe[25,26] and Sen and Thorpe[27] (ST). These authors showed that for model Hamiltonians the vibrational (as well as electronic) bands could be described exactly. Specific results for the bands have been given for four coordinated materials[25,26] such as Si and Ge and 4-2 coordinated cases,[27] such as SiO_2 and GeO_2. The key to the analytic calculations of ST is the neglect of "quantitative disorder," i.e., the calculations are carried out with the assumption that each A atom has perfect tetrahedral coordination, each X atom has the same A-X-A angle, and the Hamiltonian contains only nearest-neighbor A-X central forces with the same force constant at each bond.

The density of states for the ST model applied to GeO_2 is shown schematically in Fig. 2(b). The spectral features are three δ-function peaks in the density of states and two bands with the band edges fixed by simple formulas in terms of the masses, central force constant, and bond angle ϕ. Two δ-function peaks are shown in Fig. 2(b) and the third is at zero frequency and is comprised of bond-bending modes which are unstable in this central force model. Despite this failure for bending modes, the ST model is quite accurate for the high-frequency modes in which we are interested. Galeener has compared the frequencies predicted by the simple expressions of the ST model with the results of the large numerical cluster calculations for SiO_2, GeO_2, and BeF_2, and he finds that the agreement is within a few percent.[10]

The lower band edge denoted by ω_1 is of particular interest here. In the ST model this band edge is precisely defined even in the disordered system. It is the lack of sensitivity of the band edge at ω_1 to disorder that leads to the correlations discussed below for Raman scattering and to the simple form of the results.

In the ST model with no quantitative disorder the spectrum can be found exactly. First, we take $\alpha'^m = \alpha'$ independent of bond m, which is an extension of the ST model to require that there is no quantitative disorder in the coefficient for coupling to light. The correlation function needed is then given by Eq. (10) with $\delta\alpha'^m = 0$. Now from Galeener we have the result that at the band edge ω_1, the atomic motion is purely SS displacement of the X atoms with every bond in the network compressed in phase, i.e.,

$$\sum_m{}' n^m \cdot u^l(t) = u_{ss} e^{i\omega_1 t}$$

independent of the site l. Secondly, the displacement pattern at every other frequency is orthogonal to that at ω_1. From these two facts it follows immediately

from Eq. (10) that $S^p(\omega)$ is a δ function at $\pm\omega_1$. The polarized Raman strength for this one mode is proportional to the number of atoms N in the scattering volume and for every other mode it is zero. The δ-function coupling to one mode of the system is a property found also for perfect crystals, but long-range periodicity has not been used in the present derivation.

The results can be cast in terms of Green's functions in a form useful later. Let us define the scalar Green's function for the SS motion

$$G_{SS}(l,l',\omega)=\sum_{kk'mm'} n_k^m G_{kk'}(l,l',\omega) n_{k'}^{m'} \quad , \tag{14}$$

and denote G_{SS} in the ST model as G_{SS}^0. The properties defined above lead to the result that

$$\sum_{ll'} G_{SS}^0(l,l',\omega)=\frac{N}{M_X}/(\omega^2-\omega_1^2) \tag{15}$$

and we also arrive at the conclusion that the polarized scattering spectrum

$$S^p(\omega)=-(\alpha)^2\frac{2\omega}{1-e^{-\beta\omega}}\,\mathrm{Im}\sum_{ll} G_{SS}^0(l,l,\omega+i0^+) \tag{16}$$

consists of δ functions at $\omega=\pm\omega_1$. This is to be contrasted with the weighted density of states

$$\rho_{SS}(\omega)=\frac{\omega}{\pi}\,\mathrm{Im}\sum_{l} G_{SS}^0(l,l,\omega+i0^+) \quad , \tag{17}$$

which is the weighted broad spectrum given in Fig. 5 of ST.[27] The difference between the two expressions results from the correlations between unlike atoms $l\neq l'$.

Let us now consider a system with quantitative disorder. One type of disorder is fluctuations in the coupling to light, termed electrical disorder by Martin and Brenig.[44] In the bond polarizability model the electrical disorder can be represented by a probability distribution $Q(\delta\alpha')$ of the variation in polarizability $\delta\alpha'$ in Eq. (9). We assume no correlations on different bonds. Quantitative disorder in the force constants and in the structure, termed mechanical disorder by Martin and Brenig, affect atomic displacements and frequencies, broadening the density of states and all correlation functions. We take into account a part of this disorder by the single-site coherent potential approximation (CPA), which has been applied extensively to disordered crystals.[15] In the present case a "single site" is an A-X-A unit and random fluctuations are considered in the "site-diagonal" force constants K_{ll} for the SS motion of an X atom relative to its two A neighbors. Coupling of neighboring units via the connecting A atoms is taken to be constant and its fluctuations are ignored. This greatly simplifies the mathematics and leads to the equations given below. In the ST central force model, fluctuations in the site-diagonal forces on an X atom can result from fluctuations in the central force constant and in the A-X-A angle θ which determines the total restoring forces in the SS and AS motion respectively. Bond-bending forces K_ϕ about the A atom not included in the ST model also give rise to random self-forces. If all dihedral angles are random it is easy to show that there is a distribution of effective restoring forces on the X atom which range from 0 to a maximum of $6\sin^2\theta K_\phi = 3.2K_\phi$ for $\theta=133°$. A zero contribution to the restoring force is for the case where the four X atoms rotate rigidly around an A atom, and the maximum contribution occurs when the angles at the A atom are distorted to a maximum degree. The important point is that with noncentral forces a distribution of dihedral angles causes a distribution in restoring forces.

In this paper we include all mechanical disorder by a distribution of self-force constants $P(K_{ll})$ with no correlation of the fluctuations in K_{ll} on different sites. The CPA solution gives correlation functions of the disordered system in terms of a site-diagonal self-energy $\Sigma_{ll}(\omega)\equiv\Sigma^{\mathrm{CPA}}(\omega)$ chosen to represent the fluctuating K_{ll} forces. The CPA Green's function is the zeroth order Green's function G^0 with ω^2 corrected by the self-energy Σ, i.e.,

$$G^{\mathrm{CPA}}(l,l',\omega)=G^0(l,l',[\omega^2-\Sigma(\omega)]^{1/2}) \quad . \tag{18}$$

The CPA solution for the optimal self-energy is given by [see, e.g., Ref. 15, Eq. (3.65)]

$$\int dK\,P(K)\frac{[K-\Sigma^{\mathrm{CPA}}(\omega)]}{\{1-[K-\Sigma^{\mathrm{CPA}}(\omega)]G^{\mathrm{CPA}}(l,l,\omega)\}}=0 \quad . \tag{19}$$

Equation (19) is in principle a very complex matrix equation because in the general case K, Σ, and G are all nondiagonal matrices in the various types of atomic displacements. The equations simplify enormously if we make the approximation that only SS motions are included in Eq. (19). Then Eq. (19) reduces to a scalar equation where all quantities involve only SS motion. The solution for $\Sigma(\omega)$ is given completely in terms of the single distribution $P(K)$ and the scalar site diagonal G_{SS}^0 which is the Hilbert transform of the weighted SS density of states ρ_{SS}^0 in the ST model. This approximation is justified by the work of ST which shows (see their Fig. 5) that for large bond angles $\sim 135°$, the lowest band is essentially completely comprised of SS motion. At frequencies near the lowest band edge ω_1 the mixture of other degrees of freedom by the random forces will lead to only small corrections. It is important to note, however, that in some glasses (e.g., SiO_2) bond-bending modes are found experimentally to occur in this frequency range. That situation leads to extra broaden-

ing due to coupling with these modes not included here. Nevertheless the major conclusions remain unchanged.

The polarized Raman spectrum involves the sum over atoms and bonds given in Eq. (8). The sum is in general complicated if there is correlation of $\delta\alpha'^m$ on different sites or with the fluctuations in the force constants K_{ll}. We will give explicit results in the absence of any such correlations and will merely mention the effects of these correlations. With the above approximations, fluctuations in $\delta\alpha'^m$ cancel in the sums except for single-site contributions and

$$S^p(\omega) = -\frac{2\omega}{1-e^{-\beta\omega}}\left[(\alpha')^2\sum_{ll'}\mathrm{Im}G^{\mathrm{CPA}}(l,l',\omega) + \langle(\delta\alpha')^2\rangle\sum_{l}\mathrm{Im}G^{\mathrm{CPA}}(l,l,\omega)\right]$$

$$= (2\omega/1-e^{-\beta\omega})(N/M_X)((\alpha')^2\,\mathrm{Im}\{-\omega/[\omega^2-\omega_1^2-\Sigma^{\mathrm{CPA}}(\omega)]\} + \langle(\delta\alpha')^2\rangle\pi\rho^{\mathrm{CPA}}) \quad . \tag{20}$$

Here G^{CPA} is the SS Green's function and ρ^{CPA} the SS-weighted CPA density of states defined in terms of the self-energy. The final line in Eq. (20) follows from Eqs. (15) and (17) and shows that the spectrum is a sum of a broadened δ function associated with the band edge plus the contribution from the electrical disorder $\delta\alpha'$ which is proportional to the total SS density of states. Because the spectral functions in the last line of Eq. (20) are normalized, the integrated weight for the two contributions is in the ratio $\langle(\delta\alpha')^2\rangle/\alpha'^2$.

If there are additional correlations among the $\delta\alpha'^m$ on different bonds, the second term is modified and is not simply the density of states, and if there are correlations of $\delta\alpha'^m$ and K_{ll} then there are cross terms giving interference between the two types of contributions in Eq. (20). The interference could take the form of a broadened Fano effect and could lead to either constructive or destructive interference between the two parts.

Evaluation of Eq. (20) requires the weighted density of $\rho^0_{\mathrm{SS}}(\omega)$. The simple shape for $\rho^0_{\mathrm{SS}}(\omega)$ given by ST suggests that it is adequately represented by a smooth featureless shape, and we will choose the parabolic density of states[44] for which the solutions for $\Sigma(\omega)$ can be found analytically. The site-diagonal Green's function for this spectrum is

$$G^0_{\mathrm{SS}}(l,l,\omega) = (4/W^4)\{(\omega^2-\omega_0^2) + [(\omega^2-\omega_0^2)^2 - W^4]^{1/2}\} \tag{21}$$

for a band extending from $(\omega_0^2 - W^2)^{1/2}$ to $(\omega_0^2 + W^2)^{1/2}$. This form has often been applied as an approximation to crystalline densities of states.[14,45] The second quantity which must be fixed is the distribution $P(K)$. We have chosen a form which is convenient and allows analytic solutions

$$P(K) = (2\sigma^3/\pi)/(K^2+\sigma^2)^2 \quad . \tag{22}$$

This distribution has the virtue that it decreases faster than a Lorentzian at large K, giving a distribution appropriate for a continuously disordered system such as a glass.

The solution of Eqs. (19), (21), and (22) can be cast in the form of a complex third-order polynomial in G^{CPA}. The steps involved are carrying out the integrals over K by contour integration and noting that Σ^{CPA} obeys the relation

$$\Sigma^{\mathrm{CPA}} = \omega^2 - \omega_0^2 - (\tfrac{1}{8}W^2)G^{\mathrm{CPA}} - 2/G^{\mathrm{CPA}} \quad . \tag{23}$$

The density of states for the physical root of the polynomial is shown in Fig. 3 for several values of σ/W^2. There is also shown the first term in Eq. (20) for the polarized Raman scattering. The results for $\sigma = 0$ give the sharp band edge and δ-function Raman response if there is no quantitative disorder. The most important result is that the polarized Raman scattering spectrum is qualitatively modified from the density of states; even for very large quantitative broadening, the peak in the Raman spectrum is clearly shifted from that of the density of states and is associated with the edge of the density of states.

In Fig. 4 we show the isotropic Raman intensity $I_p(\omega)$ for GeO_2 derived from the data of Fig. 2 and using Eq. (13). We see that $I_p(\omega)$ is essentially zero

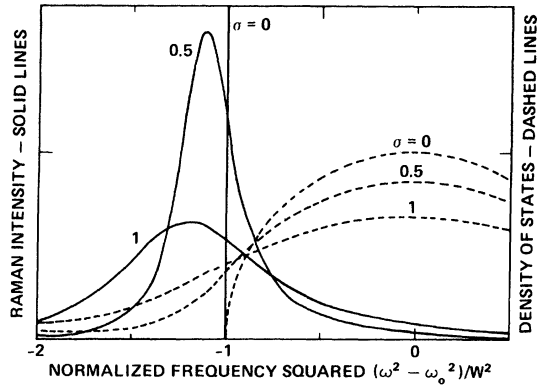

FIG. 3. Calculated densities of states (– – –) and polarized Raman spectra (——) from Eq. (19) and the first term in Eq. (20). The spectrum is given as a function of ω^2 for various values of the broadening σ. We see that even for large σ, on the order of the bandwidth, the Raman peak is still clearly distinct from the peak in the density of states.

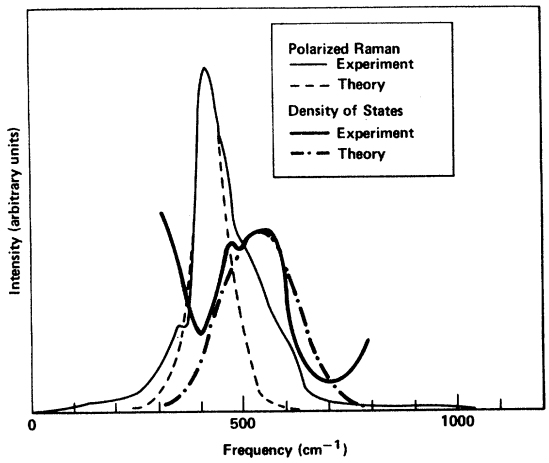

FIG. 4. Polarized Raman spectrum of GeO_2 from the data given in Fig. 2 compared with the shape predicted by the present theoretical calculations with parameters described after Eq. (23). We also show the theoretical density of states compared to a portion of the experimental density of states given in Fig. 2.

everywhere except in the band of modes identified as SS and we see that it has a peaked, asymmetrically broadened form. We also give a portion of the density of states from Fig. 2(c) to show clearly the difference between the polarized scattering and the density of states. The dotted line in Fig. 4 is the result of our calculations with a band centered at $\omega_0 = 540$ cm^{-1}, with $W = 313$ cm^{-1} so that the lower edge is at 440 cm^{-1}, and with a broadening $\sigma = 0.5W^2$, chosen to fit the observed Raman peak. Here we have set $\delta\alpha^m = 0$. We see that the theoretical results describe the observed spectrum very well while also giving a reasonable facsimile of the observed density of states. The experimental Raman spectrum exceeds the predicted spectrum in the region of the band, and is in qualitative agreement with the second term of Eq. (20) which gives the scattering due to random electrical disorder $\delta\alpha^m$. The present results can also be compared with a-SiO_2,[2] where there is also a strong polarized Raman peak. In that case, however, other bond-bending modes occur in the same frequency range broadening the Raman peak and obscuring the relation to the band edge.

The magnitude of the random forces may be compared with that from accountable sources. Since the effective self-force constant $K_{II} \sim K_r(1+\cos\theta)$, a variation in the A-X-A angle θ causes a fluctuation $dK_{II}/d\theta \sim 2.3K_{II}$. Thus

$$\langle dK_{II}^2\rangle^{1/2}/K_{II} = \sigma/\omega_1^2 \sim 0.5(313/440)^2 \sim 0.25$$

would be given by a variation in θ with $\langle d\theta^2\rangle^{1/2} = 0.25/2.3 \sim 0.1$ rad ~ 6 deg, which is a reasonable variation. Alternatively, such fluctuations could be caused by angular forces as described above, where we showed qualitatively that random dihedral angles would give a spread of effective force constants of $\sim 3.2K_\phi/3$. Using Galeener's estimate[10] of K_ϕ/K_r (β/α in his notation) of ~ 0.1, one finds

$$\langle dK_{II}^2\rangle^{1/2}/K_{II} \sim K_\phi/K_r(1+\cos\phi) \sim 0.3 \ .$$

These estimates show that the value of σ chosen in our model calculations is physically reasonable.

We have shown in Sec. III that differences in the depolarized spectrum from the density of states would be evidence for angular correlations in the glass. However, the depolarized spectrum for GeO_2 shown in Fig. 2(a) mimics the total density of states as was discussed in Sec. II. This indicates that in GeO_2 the assumption of a random network is in qualitative agreement with the Raman data.

V. OTHER SYSTEMS: PHONONS AND ELECTRONS

Our general results apply also to networks with different local order. Of particular note is P_2O_5 which consists of a pyramidal P with one strongly bound isolated O neighbor and three O neighbors which bridge to other P atoms.[8] Experiment shows two strong polarized Raman peaks.[8] Galeener and Mikkelsen[8] show that the lower peak is the symmetric in-phase motion of all the bridging atoms with the corresponding opposite symmetric displacement of the P=O units. This is a band edge for symmetric stretching vibrations, as shown in the recent work of Thorpe and Galeener,[25] analogous to that in the AX_2 glasses. Exactly the same analysis applies also to As_2O_3-type glasses where a P=O unit is replaced by an As. This suggests that the strong highly peaked polarized Raman mode in As_2O_3 is also caused by correlated symmetric motions and is associated with a band edge, essentially as described in Ref. 7.

Another case in which the experimental results show clearly a striking difference between polarized Raman and the density of states is amorphous As.[11,12] The HV Raman spectrum is essentially identical to the density of states[11] and the HH spectrum looks like a sum of a term proportional to the density of states and a very sharp additional peak at the band edge. The additional peak is more intense and sharper in annealed bulk glasses than in sputtered films.[11,12] This is the behavior predicted by Eq. (20) if the quantitative disorder is smaller in the bulk glass. Numerical calculations[46] have been carried out for amorphous As, however, the nature of the modes is not given. It is plausible, but not proved, that the lower band edge corresponds to the in-phase As symmetric stretching mode just as is the case in tetrahedral AX_2 and pyramidal A_2X_3 glasses. Amorphous P also has an apparently analogous polarized peak,[13] and in addition has a richer structure in polarized and

depolarized spectra, suggesting greater intermediate-range order than in a-As.

An interesting prediction for electronic states in glasses can be made following the arguments above. The counterpart of the symmetric vibrational modes are the symmetric s electronic states. Indeed, Sen and Thorpe derived their results for AX_2 vibrational modes by the equivalence to s and p electron states[25,26] in a tetrahedral amorphous semiconductor such as a-Si. The bottom of the SS vibrational band corresponds exactly to the bottom of the s electronic band in a-Si. The experiment which can probe correlated electronic states in a way similar to the manner in which polarized Raman probes the vibrational states is angular-resolved photoemission with the energy analyzers set to accept only $k \approx 0$ electrons. Then the observed spectrum is the imaginary part of the one-electron Green's function[15,38,39] summed over all atoms

$$G_k(\omega) = \sum_{ll'} e^{ik(R_l - R_{l'})} \langle\langle b_l^\dagger ; b_{l'} \rangle\rangle_\omega \ , \tag{24}$$

where $b_l^\dagger$ is an electron creation operator at site l. All the arguments used in Sec. IV apply here also and the spectrum will be weighted toward the band edge exactly as in Fig. 3. Since the bandwidth[47] for the s-like states is of order 5 eV in a-Si, the shift in the spectrum should be clearly visible. For large k, however, the photoemission spectrum should be close to the density of states. The counterpart of Raman selection rules is that the electron velocity should be parallel to the photon electric polarization to see this spectral signature. In the perpendicular geometry our results predict a spectrum close to the density of states. To our knowledge no theoretical suggestions or experimental tests of interesting angular-dependent photoemission spectra have been given previously.

In conclusion, we have shown that polarized Raman scattering plays a special role in glasses and is sensitive to correlations in the motion of nearby atoms. The central force model of Sen and Thorpe[27] for AX_2 glasses lends itself to an analytic form for the correlated motion taking into account the topological disorder. It predicts that the *polarized* Raman peak is associated with an *edge* of a band of vibrational states, in full agreement with experimental results on GeO_2. The depolarized scattering on the other hand is shown to mimic the density of states unless there is strong angular correlation between nearby bonds, i.e., well-defined intermediate-range order. Much evidence indicates that the same features hold in many other glasses. By using the mapping of the model to electronic states,[25–27] we use the same results to predict structure in angular-resolved photoemission from a-Si and similar disordered materials.

ACKNOWLEDGMENTS

In the early stages of this work, we benefited greatly from conversations with P. N. Sen and M. F. Thorpe. We also want to acknowledge a useful conversation with Y. Petroff on photoemission. The work of one of us (F.L.G.) was supported in part by the Office of Naval Research.

[1]For a review of literature, see J. Wong and C. A. Angell, *Glass Structure by Spectroscopy* (Marcel-Dekker, New York, 1976).

[2]F. L. Galeener and G. Lucovsky, Phys. Rev. Lett. 37, 1474 (1976).

[3]V. V. Obukhov-Denisov, N. N. Soboler, and V. P. Cheremisinov, Opt. Spectrosc. (USSR) 8, 267 (1960).

[4]F. L. Galeener, G. Lucovsky, and R. Geils, Solid State Commun. 25, 405 (1978).

[5]G. Lucovsky, F. L. Galeener, R. C. Keezer, R. Geils, and H. Six, Phys. Rev. B 10, 5134 (1974).

[6]C. A. Angell and J. Wong, J. Chem. Phys. 53, 2053 (1970); F. L. Galeener and J. C. Mikkelsen, Jr., A. C. Wright, R. N. Sinclair, J. A. E. Desa, and J. Wong, J. Non-Cryst. Solids 42, 23 (1980).

[7]F. L. Galeener, G. Lucovsky, and R. Geils, Phys. Rev. B 19, 4251 (1979).

[8]F. L. Galeener and J. C. Mikkelsen, Jr., Solid State Commun. 30, 505 (1979).

[9]W. L. Konijnendijk and J. M. Stevels, J. Non-Cryst. Solids 18, 307 (1975); F. L. Galeener, G. Lucovsky, and J. C. Mikkelsen, Jr., Phys. Rev. B 22, 3983 (1980).

[10]F. L. Galeener, Phys. Rev. B 19, 4292 (1979).

[11]J. S. Lannin, Phys. Rev. B 15, 3863 (1977).

[12]R. J. Nemanich, G. Lucovsky, W. Pollard, and J. D. Joannopoulos, Solid State Commun. 26, 137 (1978).

[13]J. S. Lannin and B. V. Shanabrook, Solid State Commun. 28, 497 (1978).

[14]F. L. Galeener, A. J. Leadbetter, and M. W. Stringfellow (unpublished). See also A. J. Leadbetter and D. Litchinsky, Discuss. Faraday Soc. 50, 62 (1970).

[15]R. J. Elliot, J. A. Krumhansl, and P. L. Leath, Rev. Mod. Phys. 46, 465 (1974).

[16]R. J. Bell, in *Methods in Computational Physics*, edited by G. Gilat (Academic, New York, 1976), p. 215.

[17]A. C. Wright and A. J. Leadbetter, Phys. Chem. Glasses 17, 122 (1976).

[18]G. Lucovsky and R. M. Martin, J. Non-Cryst. Solids 8, 185 (1978).

[19]S. Brauer, Phys. Rev. B 11, 3173 (1975).

[20]R. J. Bell and P. Dean, Discuss. Faraday Soc. 50, 55 (1970).

[21]R. J. Bell and D. C. Hibbins-Butler, J. Phys. C 9, 2955 (1976).

[22]R. Alben, D. Weaire, J. E. Smith, and M. Brodsky, Phys. Rev. B 11, 2271 (1975).

[23]K. Kulas and M. F. Thorpe, in *Structure and Excitation of Amorphous Solids—1976,* edited by G. Lucovsky and F. L. Galeener, AIP Conf. Proc. No. 31 (AIP, New York, 1976), p. 251.
[24]R. B. Laughlin and J. D. Joannopoulos, Phys. Rev. B 16, 2942 (1977).
[25]D. Weaire and M. F. Thorpe, Phys. Rev. B 4, 2508 (1971).
[26]M. F. Thorpe and D. Weaire, Phys. Rev. B 4, 3518 (1971).
[27]P. N. Sen and M. F. Thorpe, Phys. Rev. B 15, 4030 (1977).
[28]A. J. Leadbetter and A. C. Wright, J. Non-Cryst. Solids 7, 37 (1972).
[29]A. C. Wright, Adv. Struct. Res. Diffr. Methods 5, 1 (1974)
[30]R. J. Bell and P. Dean, Philos. Mag. 25, 1381 (1972).
[31]J. B. Bates, J. Chem. Phys. 56, 1970 (1972).
[32]J. B. Bates, J. Chem. Phys. 56, 1528 (1972).
[33]J. F. Scott and S. P. S. Porto, Phys. Rev. 161, 903 (1967).
[34]J. F. Scott, Phys. Rev. B 1, 3488 (1970).
[35]M. F. Thorpe and F. L. Galeener, Phys. Rev. B 22, 3078 (1980).
[36]L. D. Landau and I. Lifshitz, *Electrodynamics of Continuous Media* (Pergamon, New York, 1960), p. 390.
[37]B. J. Berne and R. Pecora, *Dynamic Light Scattering* (Wiley, New York, 1976).
[38]P. C. Martin, *Measurements and Correlation Functions* (Gordon and Breach, New York, 1968).
[39]S. Doniach and E. H. Sondheimer, *Green's Functions for Solid State Physics* (Benjamin, Reading, Mass., 1974).
[40]F. L. Galeener and P. N. Sen, Phys. Rev. B 17, 1928 (1978).
[41]R. Shuker and R. W. Gammon, Phys. Rev. Lett. 25, 222 (1970).
[42]D. A. Long, *Raman Spectroscopy* (McGraw-Hill, New York, 1977), Chap. 3.
[43]D. A. Kleinman and W. G. Spitzer, Phys. Rev. 125, 16 (1962).
[44]A. J. Martin and W. Brenig, Phys. Status Solidi B 64, 163 (1974).
[45]J. Hubbard, Proc. R. Soc. London Ser. A 281, 401 (1963)
[46]W. B. Pollard and J. D. Joannopoulos, Phys. Rev. B 17, 1778 (1978).
[47]R. Pollak, L. Ley, S. Kowalcyzk, D. A. Shirley, J. Joannopoulos, D. J. Chadi, and M. L. Cohen, Phys. Rev. Lett. 29, 1103 (1973).